

# Magnetic Hand Tracking for Human-Computer Interface

Yinghong Ma<sup>1,2</sup>, Zhi-Hong Mao<sup>2</sup>, Wenyan Jia<sup>2</sup>, Chengliu Li<sup>2</sup>, Jiawei Yang<sup>1</sup>, and Mingui Sun<sup>2</sup>

<sup>1</sup>Information Science Institute, State Key Laboratory of Integrated Service Networks, Xidian University, Xi'an, Shaanxi 710071, China

<sup>2</sup>Laboratory for Computational Neuroscience, Department of Neurosurgery and Department of Electrical and Computer Engineering, University of Pittsburgh, Pittsburgh, PA 15260 USA

**Hand motion tracking is useful in human-computer interface and many other applications requiring human-machine interactions. In this work, permanent magnets and contactless magnetic sensors are used to track finger motion. A magnet patch is affixed to each fingernail to mark the location and orientation of the fingertip. When fingers move, the combined magnetic fields produced by the magnets at fingertips are recorded by a set of magnetic sensors around a wristband. The recorded data from the sensors are utilized to calculate the magnets' locations and orientations, which can provide estimate of the hand posture based on a geometric hand model.**

**Index Terms**—Hand tracking, human-computer interface, magnetic marker, wireless motion capture.

## I. INTRODUCTION

**A**LTHOUGH computers have become faster, smaller, and ubiquitous, the keyboard and the pointing/selecting mouse as main computer interface devices have not changed for decades. While these devices are quite suitable in desktop computers and laptops, they are inefficient, cumbersome, and inconvenient when used in portable mobile devices. For example, the keyboard, which evolved from the classical mechanical typewriter, consists of up to 110 individually marked keys and switches mounted on a printed circuit board. The size of the keyboard cannot be reduced aggressively without sacrificing operability. In addition, constant keyboard typing causes fatigue or even chronic injuries to users, such as carpal tunnel syndrome, hand and eye fatigue, and neck and back strain.

Many attempts have been made to replace the conventional physical keyboard and mouse [1]–[4]. Voice recognizers have been used to provide instructions to the computer without hand motion [1], [2]. Projection-based devices project a keyboard on a flat surface and key strokes of all ten fingers on the virtual keyboard can be identified [3]. Virtual keyboards, which can be activated by touching screen using a finger or a stylus, have been used in cell phones, GPS navigators, cars, medical instruments and other computerized systems [4]. Although these methods provide alternatives to the keyboard/mouse, they are either suitable only for specific applications or limited by low information rates. The method based on voice recognition provides a convenient human-computer interface. However, this method is prone to error due to the environmental voice interferences. Although the projection based systems require no hand attachments, it requires a suitable location to place a projector and suffers from the occlusion problem. The screen based virtual keyboard is inexpensive and requires no external input device (with an occasional exception of a stylus). However, such a virtual keyboard

occupies valuable screen space and the rate of information input is often very low.

If human finger motions and hand postures, which carry information, can be observed by a simple apparatus, it will become possible that the motion of the fingers and palm in free space without touching any objects can be used to operate the computer. This will allow rapid and convenient communication with computers and enable more ubiquitous computer applications in people's daily lives. Different methods have been proposed to track hand motion information [5]–[9]. For example, camera-based systems rely on image processing approach to obtain finger positioning and to perform rudimentary finger tracking [5]. Glove-based methods use sensors to measure the acceleration or strain of fingers during movement, or the pressure at the finger when being touched [5], [6]. However, the method using image processing suffers from dead angles, while the glove-based method requires complex components and is uncomfortable and obstructive when being utilized. There are also reports on electro-myogram (EMG)-based methods [7] and magnetic methods [8], [9]. However, the accuracy of the EMG method is very low due to the complex muscular interactions, while the current magnetic systems either require a large magnetic object as a marker or electric wire connections.

In this work, we report a magnetic hand motion tracking system using small magnets (which can be made in the form of artificial nails) and an electronic wristband. This system leverages advanced design of magnetic flux sensors and recent research on hand-based communication. It is wireless, portable, unobstructive, and convenient. With specifically designed software that captures hand gestures, this system can be used in computer input, camera operation, and many other applications, such as controlling a wheelchair, robot, or portable aircraft by hand gestures, engaging in a conversation by generating synthetic speech produced by a hand code, and controlling rigidity and tremor in patients with Parkinson's disease by computer "reading" of involuntary hand movement.

The rest of this paper is organized as follows. Section II describes the architecture of our hand motion tracking system. Section III presents a hand tracking algorithm based on a hand geometric model and a mathematical model of the magnetic field produced by a permanent magnet. Section IV evaluates the

Manuscript received May 25, 2010; accepted August 30, 2010. Date of current version April 22, 2011. Corresponding author: M. Sun (e-mail: drsun@pitt.edu).

Color versions of one or more of the figures in this paper are available online at <http://ieeexplore.ieee.org>.

Digital Object Identifier 10.1109/TMAG.2010.2076401

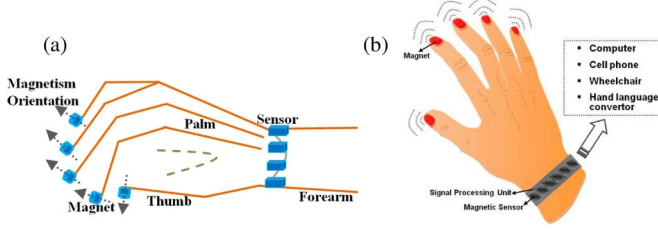


Fig. 1. Structure of the magnetic hand motion tracking system.

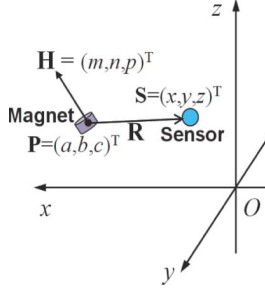


Fig. 2. Magnetic dipole model of a magnet.

performance of the prototype system through experiments. Section V concludes this paper and presents the directions of our future work.

## II. COMPONENTS AND STRUCTURE OF THE SYSTEM

Fig. 1 shows the structure of the magnetic hand motion tracking system. The system consists of two major components: a set of permanent magnets (in the form of artificial fingernails) and an electronic wristband. A combined magnetic field is established by the magnets and varies with the finger movements. Multiple magnetic sensors, which are distributed around the wrist, detect magnetic flux at their predetermined positions. The measured data are used to inversely calculate hand postures.

## III. HAND TRACKING METHOD

In our system, hand tracking is divided into two computational steps. The first step estimates the locations and orientations of the magnets and the fingertips from the measured flux densities, and the second step reconstructs the finger postures from the locations and orientations of the fingertips based on a geometric model of fingers.

### A. Magnet Model and Localization/Orientation of Fingertips

Fig. 2 shows a magnet located at  $\mathbf{P} = (a, b, c)^T$  with orientation  $\mathbf{H} = (m, n, p)^T$ . Let  $\mathbf{R} = (x - a, y - b, z - c)^T$  represent the relative location of a point  $\mathbf{S} = (x, y, z)^T$  with respect to the magnet. The magnetic flux density at  $\mathbf{S}$  is determined by

$$\mathbf{B} = \frac{\eta\mu}{4\pi} \left( \frac{3(\mathbf{H} \cdot \mathbf{R})\mathbf{R}}{R^5} - \frac{\mathbf{H}}{R^3} \right) \quad (1)$$

where  $R$  is the Euclidean norm of  $\mathbf{R}$  (i.e.,  $R = \|\mathbf{R}\|$ ),  $\mu$  the medium permeability, and  $\eta$  the magnetic strength of the magnet [9].

Assume that there are  $K$  magnets and  $N$  magnetic sensors, with the predetermined position of  $n$ th sensor at  $\mathbf{S}_n = (x_n, y_n, z_n)^T$ ,  $1 \leq n \leq N$ . The magnetic flux density at the  $n$ th sensor can be calculated by

$$\begin{aligned} \mathbf{B}_n &= \sum_{k=1}^K \frac{\eta_k\mu}{4\pi} \left( \frac{3(\mathbf{H}_k \cdot \mathbf{R}_{nk})\mathbf{R}_{nk}}{R_{nk}^5} - \frac{\mathbf{H}_k}{R_{nk}^3} \right) \\ &\equiv \sum_{k=1}^K \lambda_k \mathbf{f}(\mathbf{H}_k, \mathbf{P}_k) \end{aligned} \quad (2)$$

where  $\mathbf{R}_{nk} = \mathbf{S}_n - \mathbf{P}_k$  and  $\lambda_k = (\eta_k\mu)/(4\pi)$ .

The location and orientation of a fingertip are represented by those of the magnet on the fingertip, respectively. To localize the fingertip, we need to determine  $\{\mathbf{H}_k, \mathbf{P}_k\}$  using the measured magnetic flux densities. In the presence of noise, the simultaneous measurements at the sensors can be represented by

$$\begin{aligned} \tilde{\mathbf{M}} &\equiv [\tilde{\mathbf{B}}_1 \dots \tilde{\mathbf{B}}_N]^T \\ &= \begin{bmatrix} \mathbf{f}_{11}(\mathbf{H}_1, \mathbf{P}_1) & \dots & \mathbf{f}_{1K}(\mathbf{H}_K, \mathbf{P}_K) \\ \vdots & \dots & \vdots \\ \mathbf{f}_{N1}(\mathbf{H}_1, \mathbf{P}_1) & \dots & \mathbf{f}_{NK}(\mathbf{H}_K, \mathbf{P}_K) \end{bmatrix} \times \begin{bmatrix} \lambda_1 \\ \vdots \\ \lambda_K \end{bmatrix} + \mathbf{w} \\ &\equiv \mathbf{F}(\{\mathbf{H}_k, \mathbf{P}_k\})\boldsymbol{\lambda} + \mathbf{w} \end{aligned} \quad (3)$$

where  $\mathbf{w}$  denotes the  $N \times 1$  noise vector.

We use a least-squares (LS) dipole fitting method to estimate  $\{\mathbf{H}_k, \mathbf{P}_k\}$  from  $\tilde{\mathbf{M}}$ . Define the cost function as

$$J(\{\mathbf{H}_k, \mathbf{P}_k\}, \boldsymbol{\lambda}) \equiv \|\tilde{\mathbf{M}} - \mathbf{F}(\{\mathbf{H}_k, \mathbf{P}_k\})\boldsymbol{\lambda}\|^2. \quad (4)$$

The following formulation is further applied to cancel the unknown parameter  $\boldsymbol{\lambda}$ , which is irrelevant to the location and orientation of the fingertip [10]:

$$\begin{aligned} J_0(\{\mathbf{H}_k, \mathbf{P}_k\}) &\equiv J|_{\boldsymbol{\lambda}=\mathbf{F}^+\tilde{\mathbf{M}}} \\ &= \|\tilde{\mathbf{M}} - \mathbf{F}(\mathbf{F}^+\tilde{\mathbf{M}})\|^2 \\ &= \|(\mathbf{I} - \mathbf{F}\mathbf{F}^+)\tilde{\mathbf{M}}\|^2 \end{aligned} \quad (5)$$

where  $\mathbf{F}^+$  denotes the pseudo inverse of  $\mathbf{F}(\{\mathbf{H}_k, \mathbf{P}_k\})$ . Then  $\{\mathbf{H}_k, \mathbf{P}_k\}$  can be computed by minimizing  $J_0$  via an iterative numerical optimization procedure.

### B. Hand Model and Reconstruction of Hand Postures

A hand geometric model [12], without considering the movement of abduction and adduction, is utilized to derive the relation between the hand postures and the location/orientation of fingertips. This model is applicable to all fingers except the thumb which requires a different model (to be described elsewhere). According to the hand anatomy [11], each of the four fingers consists of four bones, i.e., distal phalange, middle phalange, proximal phalange, and metacarpal, which are connected by the distal interphalangeal (DIP), proximal interphalangeal (PIP), and metacarpophalangeal (MCP) joints, respectively (see Fig. 3). The posture of finger  $k$  ( $k = 1-4$  with 1 for the index finger and 4 for the pinky finger) is determined by the angles of the finger joints and wrist. For finger  $k$ , the angles of the wrist,

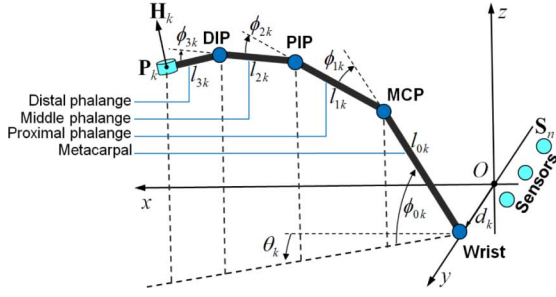


Fig. 3. Model of the index, middle, ring, or pinky finger.

MCP, PIP, and DIP joints are denoted  $\phi_{0k}$ ,  $\phi_{1k}$ ,  $\phi_{2k}$ , and  $\phi_{3k}$ , respectively. The location and orientation of the fingertip of finger  $k$  are related to the finger posture by

$$\begin{aligned} a_k &= [l_{0k} \cos(\phi_{0k}) + l_{1k} \cos(\phi_{0k} - \phi_{1k}) \\ &\quad + l_{2k} \cos(\phi_{0k} - \phi_{1k} - \phi_{2k}) \\ &\quad + l_{3k} \cos(\phi_{0k} - \phi_{1k} - \phi_{2k} - \phi_{3k})] \cos(\theta_k) \\ &\equiv \Gamma_a(\phi_{0k}, \phi_{1k}, \phi_{2k}, \phi_{3k}) \end{aligned} \quad (6)$$

$$\begin{aligned} b_k &= [l_{0k} \cos(\phi_{0k}) + l_{1k} \cos(\phi_{0k} - \phi_{1k}) \\ &\quad + l_{2k} \cos(\phi_{0k} - \phi_{1k} - \phi_{2k}) \\ &\quad + l_{3k} \cos(\phi_{0k} - \phi_{1k} - \phi_{2k} - \phi_{3k})] \sin(\theta_k) + d_k \\ &\equiv \Gamma_b(\phi_{0k}, \phi_{1k}, \phi_{2k}, \phi_{3k}) \end{aligned} \quad (7)$$

$$\begin{aligned} c_k &= l_{0k} \sin(\phi_{0k}) + l_{1k} \sin(\phi_{0k} - \phi_{1k}) \\ &\quad + l_{2k} \sin(\phi_{0k} - \phi_{1k} - \phi_{2k}) \\ &\quad + l_{3k} \sin(\phi_{0k} - \phi_{1k} - \phi_{2k} - \phi_{3k}) \\ &\equiv \Gamma_c(\phi_{0k}, \phi_{1k}, \phi_{2k}, \phi_{3k}) \end{aligned} \quad (8)$$

$$\begin{aligned} m_k &= \cos(\pi/2 + \phi_{0k} - \phi_{1k} - \phi_{2k} - \phi_{3k}) \cos(\theta_k) \\ &\equiv \Gamma_m(\phi_{0k}, \phi_{1k}, \phi_{2k}, \phi_{3k}) \end{aligned} \quad (9)$$

$$\begin{aligned} n_k &= \cos(\pi/2 + \phi_{0k} - \phi_{1k} - \phi_{2k} - \phi_{3k}) \sin(\theta_k) \\ &\equiv \Gamma_n(\phi_{0k}, \phi_{1k}, \phi_{2k}, \phi_{3k}) \end{aligned} \quad (10)$$

$$\begin{aligned} p_k &= \sin(\pi/2 + \phi_{0k} - \phi_{1k} - \phi_{2k} - \phi_{3k}) \\ &\equiv \Gamma_p(\phi_{0k}, \phi_{1k}, \phi_{2k}, \phi_{3k}) \end{aligned} \quad (11)$$

where  $l_{0k}$ ,  $l_{1k}$ ,  $l_{2k}$ , and  $l_{3k}$  are the (fixed) lengths of the corresponding bones of finger  $k$ , respectively;  $\theta_k$  is the (fixed) angle between the  $x$ - $O$ - $z$  plane and the plane where finger  $k$  lies; and  $d_k$  is the (fixed)  $y$ -coordinate of the intersection of finger  $k$  and the wrist. Introducing

$$\begin{cases} \mathbf{u} \equiv (a_k, b_k, c_k, m_k, n_k, p_k)^T \\ \mathbf{v} \equiv (\phi_{0k}, \phi_{1k}, \phi_{2k}, \phi_{3k})^T \\ \Gamma(\mathbf{v}) \equiv (\Gamma_a(\mathbf{v}), \Gamma_b(\mathbf{v}), \Gamma_c(\mathbf{v}), \Gamma_m(\mathbf{v}), \Gamma_n(\mathbf{v}), \Gamma_p(\mathbf{v}))^T \end{cases}.$$

Equation (6)–(11) can be written in a compact form

$$\mathbf{u} = \Gamma(\mathbf{v}) \quad (12)$$

which associates to each value of  $\mathbf{u}$  a unique value of  $\mathbf{v}$  (a proof of uniqueness will be provided in another manuscript of the authors).

Since a closed-form solution of  $\mathbf{v}$  in terms of  $\mathbf{u}$  is difficult to obtain from the nonlinear equation (12), we use an inverse kinematics solution technique called the Jacobian Transpose al-

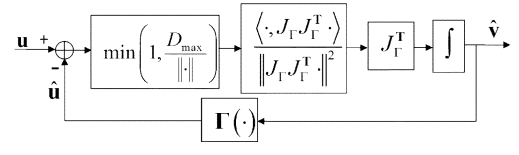


Fig. 4. Jacobian Transpose algorithm for reconstructing finger posture.

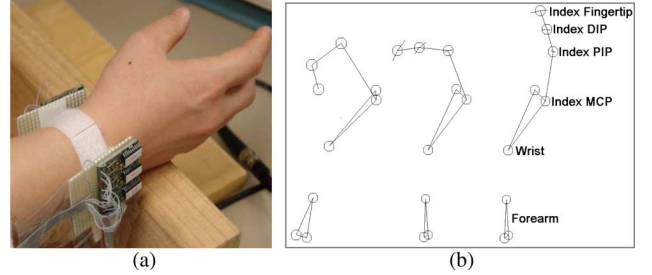


Fig. 5. (a) Prototype wristband. (b) Postures of the index finger instantaneously captured by the commercial Vicon system.

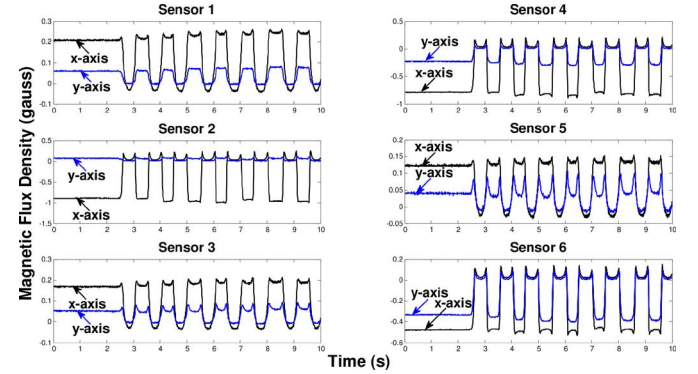


Fig. 6. Magnetic data of periodic extensions and flexions of the index finger.

gorithm [13]–[15] to compute  $\mathbf{v}$  from  $\mathbf{u}$ . The algorithm is based on the relation between the time-derivatives of  $\mathbf{u}$  and  $\mathbf{v}$

$$\dot{\mathbf{u}} = J_\Gamma(\mathbf{v})\dot{\mathbf{v}} \quad (13)$$

where  $J_\Gamma(\mathbf{v})$  is the Jacobian matrix  $\partial\mathbf{u}/\partial\mathbf{v}$ . This equation provides a linear approximation of the relation between the change in the posture of finger  $k$  and the instantaneous change in the location and orientation of the fingertip. The Jacobian Transpose algorithm gives an iterative solution of  $\mathbf{v}$  utilizing (12) and (13) by the scheme shown in Fig. 4 (algorithmic details can be found in [13]–[15]).

In Fig. 4,  $\hat{\mathbf{u}}$  is the fingertip location and orientation calculated from the updated estimate of the joint angles,  $\hat{\mathbf{v}}$ , in a single iteration.  $D_{\max}$  is the maximum step size used in the iteration.

#### IV. EXPERIMENTAL RESULTS

The index finger was chosen to test the prototype system. A commercial motion tracking system (Vicon, Los Angeles, CA) was used to track the actual finger motion. Magneto-resistive sensors (HMC1002, Honeywell International Inc.) were used in our system. Each sensor measured the magnetic field in two orthogonal axes (denoted as  $x$ -axis and  $y$ -axis, respectively). The measurement range was  $\pm 2$  gauss with resolution of  $30 \mu$  gauss and sensitivity of  $3.2 \text{ mV/V/gauss}$ .

In our experiment, a human subject was invited to do the extension and flexion movements of the index finger and keep the joints of other fingers unchanged. Fig. 5(b) shows the instan-

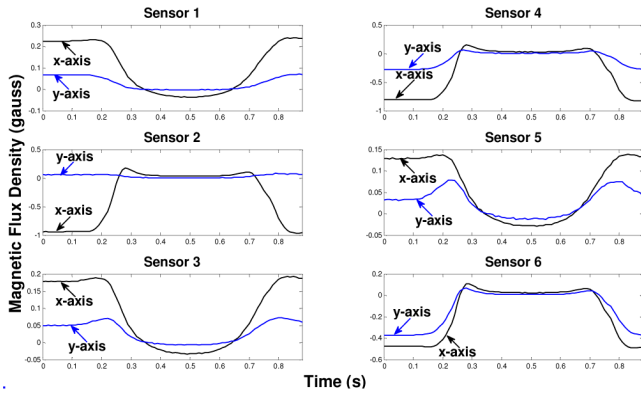


Fig. 7. Averaged magnetic data of the extension and flexion of the index finger.

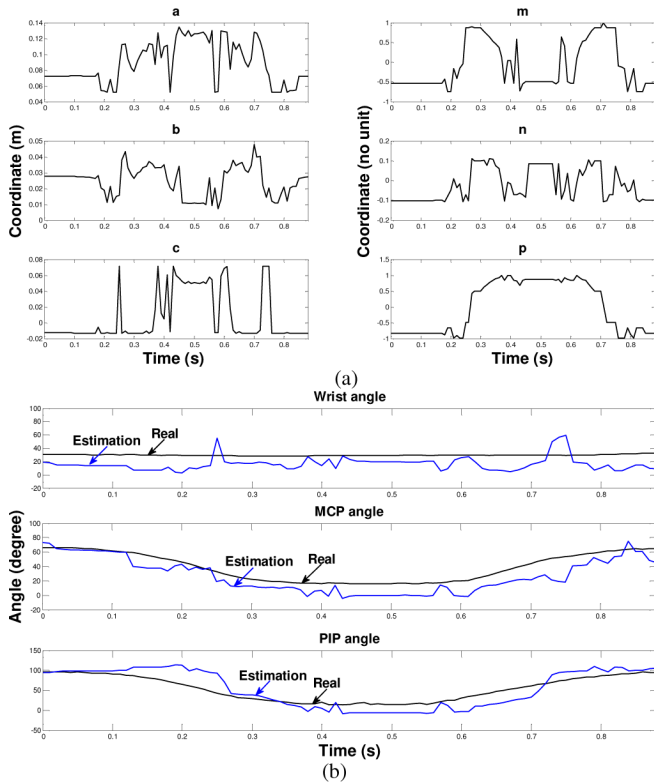


Fig. 8. (a) Tracking results of the fingertip motion of the index finger. (b) Tracking results of the finger motion.

taneously captured postures of the index finger by the Vicon system. The raw magnetic data were collected by six sensors on the prototype wristband [see Fig. 5(a)] and are shown in Fig. 6. Averaging was performed on the raw data to reduce the random noise. The de-noised data (see Fig. 7) was then used to estimate the motion of the index finger.

Fig. 8(a) shows the tracking results of the fingertip motion of the index finger. The minimization of (5) was implemented by a Pattern Search method [16], which does not require the gradient information.

In the calculation of finger postures, we used the constraint  $\phi_{3k} = (2/3)\phi_{2k}$  to reduce the dimensionality of finger articulation [17]. Fig. 8(b) shows the estimated joint-angle profiles of the index finger and compares them with the tracking results obtained by the Vicon motion tracking system. Although fluctuations were noticeable in the estimated joint-angle profiles, the

estimation based on magnetic data was reasonably consistent with the direct measurement of the joint angles.

## V. CONCLUSION

This paper reported a wireless, portable, and unobstructive hand motion tracking system for human-computer interface. A preliminary two-step hand tracking algorithm was developed. Experiments were conducted to evaluate the prototype system. Despite measurement errors, the results clearly showed that the system was able to track finger motion effectively. In future work, finite element magnetostatic analysis will be carried out to valid and improve the proposed model. Automatic detection and cancellation of unwanted external magnetic fields will also be studied to reduce noise and artifacts in the magnetic flux measurements when the system is operated near objects constructed of magnetic materials.

## ACKNOWLEDGMENT

This work was supported in part by U.S. Army Contract W81XWH-050C-0047, NIH Grant U01 HL91736, and NSF Grant CMMI-0953449.

## REFERENCES

- [1] T. Watanabe and M. Watari, "Voice input system," U.S. Patent 4641 342, Feb. 3, 1987.
- [2] M. Kolsch and M. Turk, "Keyboards without keyboards: A survey of virtual keyboards," presented at the Sensing Input for Media-Centric Syst. Symp., Santa Barbara, CA, 2002.
- [3] Virtual Devices, Inc., Pittsburgh, PA, "The Virtual Keyboard (VKPC)," 2010. [Online]. Available: <http://www.virtualdevices.net>
- [4] DSI Datotech Systems Inc., Vancouver, BC, Canada, "Multi-point touchpad," 2010. [Online]. Available: <http://www.conceptmatch.com/dsi>
- [5] Y. Wu, J. Y. Lin, and T. S. Huang, "Capturing natural hand articulation," in *Proc. Int. Conf. Comput. Vision*, 2001, pp. 426–432.
- [6] D. Won, H.-G. Lee, J.-Y. Kim, M. Choi, and M.-S. Kang, "Development of a wearable input device based on human hand-motions recognition," in *Proc. Int. Conf. Intell. Robots Syst.*, 2004, pp. 1636–1641.
- [7] J. Kim, S. Mastnik, and E. André, "EMG-based hand gesture recognition for realtime biosignal interfacing," in *Proc. Int. Conf. Intell. User Interfaces*, 2008, pp. 30–39.
- [8] K. Mitobe et al., "Development of a motion capture system for a hand using a magnetic three dimensional position sensor," presented at the ACM SIGGRAPH Res. Posters, Boston, MA, 2006.
- [9] S. Hashi, M. Toyoda, S. Yabukami, K. Ishiyama, Y. Okazaki, and K. I. Arai, "Wireless magnetic motion capture system for multi-marker detection," *IEEE Trans. Magn.*, vol. 42, no. 10, pp. 3279–3281, Oct. 2006.
- [10] S. Baillet, J. C. Mosher, and R. M. Leahy, "Electromagnetic brain mapping," *IEEE Signal Process. Mag.*, vol. 18, no. 6, pp. 20–21, Nov. 2001.
- [11] Z.-H. Mao, H.-N. Lee, R. J. Scabassi, and M. Sun, "Information capacity of the thumb and the index finger in communication," *IEEE Trans. Biomed. Eng.*, vol. 56, no. 5, pp. 1535–1545, May 2009.
- [12] Y. Ma, W. Jia, C. Li, J. Yang, Z.-H. Mao, and M. Sun, "Magnetic hand motion tracking system for human-machine interaction," *Electron. Lett.*, vol. 46, no. 9, pp. 621–623, Apr. 2010.
- [13] S. R. Buss, "Introduction to inverse kinematics with jacobian transpose, pseudoinverse and damped least squares methods," Dept. Math., Univ. California San Diego, La Jolla, CA, Oct. 2009.
- [14] W. A. Wolovich and H. Elliott, "A computational technique for inverse kinematics," in *Proc. 23rd IEEE Conf. Dec. Control*, 1984, pp. 1359–1363.
- [15] L. Sciavicco and B. Siciliano, "A solution algorithm to the inverse kinematic problem for redundant manipulators," *IEEE J. Robot. Autom.*, vol. 4, no. 4, pp. 403–410, Aug. 1988.
- [16] V. Torczon, "On the convergence of pattern search algorithms," *SIAM J. Opt.*, vol. 7, no. 1, pp. 1–25, 1997.
- [17] J. Lin, Y. Wu, and T. S. Huang, "Modeling the constraints of human hand motion," in *Proc. Workshop Human Motion*, Dec. 2000, pp. 121–126.